

Investigations on Reactivity Controlled Compression Ignition Combustion with Different Injection Strategies using Alternative Fuels Produced from Waste Resources

Arun Raj Chidambaram¹, Anand Krishnasamy^{1*}, Ganesh Duraisamy², Abul Kalam Hossain³

¹Indian Institute of Technology Madras, Chennai 600036, India,

²Anna University, Chennai 600025, India

³Aston University, Birmingham B4 7ET, United Kingdom

*Corresponding author email: anand_k@iitm.ac.in

Abstract

Reactivity-controlled compression ignition (RCCI) is a promising low-temperature combustion (LTC) strategy that results in low oxides of nitrogen (NO_x) and soot emissions while maintaining high thermal efficiency. At the same time, RCCI leads to increased unburned hydrocarbon (HC) and carbon monoxide (CO) emissions in the exhaust, particularly under low loads. The current work experimented novel port-injected RCCI (PI-RCCI) strategy to overcome the high unburned emission limitations at low load conditions in RCCI. PI-RCCI is a port injection strategy in which low-reactivity fuel (LRF) is injected using a low-pressure injector, and the high-reactivity fuel (HRF) is injected through a high-pressure common rail direct injection (CRDI) injector. The low volatile HRF is injected into a heated fuel vaporizer maintained at 180°C in the intake manifold during the suction stroke. Modifying a single-cylinder, light-duty diesel engine with the necessary intake and fuel injection systems allows engine operation in both RCCI and PI-RCCI modes. Alternative fuels from waste resources such as waste cooking oil biodiesel (WCO) and plastic waste oil (WPO) are used as the HRF and LRF fuel in RCCI and PI-RCCI. To achieve maximum thermal efficiency in RCCI, the premixed energy ratio and the start of injection of the direct-injected fuel are optimized at all load conditions. The engine performance and exhaust emissions characteristics in PI-RCCI are compared with RCCI as a baseline reference. The results show a 70% and 48% reduction in CO and HC emissions, respectively, in PI-RCCI than in RCCI. Further, the brake thermal efficiency (BTE) was enhanced by around 20%, and the brake-specific fuel consumption (BSFC) was reduced by 13% in PI-RCCI. The NO_x emissions decreased without any considerable changes in soot emission in PI-RCCI. The current study shows that fuels derived from waste resources can be used in RCCI and PI-RCCI modes with better engine performance and lower emissions.

Keywords: Plastic waste oil, Waste cooking oil, RCCI, PI-RCCI, Engine performance, Reduced Emissions

1. Introduction

Plastic production and consumption in the globe increased rapidly over the years due to its applications in a wide range of sectors [1]. The continuous use of plastics causes a significant increase in plastic waste in landfill, which consume a lot of land space and pollute water bodies, contributing to severe environmental problems [1]. Recycling plastic waste causes water pollution, and the separation process is laborious and expensive, reducing sustainability [2]. Plastic waste contributes to a significant fraction of municipal solid wastes, the segregation of plastics is a tedious process, and as a result, they accumulate land space [3]. Typical waste management practices, like landfilling and incineration, are unsustainable for disposing plastic waste as they cause land and water pollution [4]. One way to efficiently handle plastic waste is energy extraction through incineration, gasification, and pyrolysis, which is sustainable and economically viable. [4,5]. Incineration of plastic waste release pollutants into the air [7].

Pyrolysis is one of the most effective and sought-after methods to recover energy from discarded plastics. In pyrolysis, the plastic waste is heated without oxygen at temperatures of 300 to 900 °C, which results in the thermal degradation of plastic waste and produces liquid oil, char and syngas [8]. Pyrolysis transforms low-energy-density materials into high-value chemicals and reduces environmental hazards compared to conventional energy recovery methods [9]. The characteristics of the fuel obtained from plastic wastes through pyrolysis depend upon the process temperature, catalyst and type of plastic used as feedstock [10]. Producing liquid fuels from plastic waste by pyrolysis can be a sustainable solution for effectively managing plastic waste.

Conventional heterogeneous and high-temperature combustion produces high NO_x and soot emissions from diesel engines [11]. The low-temperature combustion (LTC) strategies were widely studied due to low NO_x and soot emission potential combined with high thermal efficiency [12]. Maintaining fuel-air equivalence ratios below two and in-cylinder combustion gas temperatures lower than 2200 K allows LTC modes to eliminate NO_x and soot formation zones [13]. Among the different LTC strategies, RCCI received extensive research to date [14–16]. Though HCCI and PCCI combustion modes are clean and efficient, their operating range is restricted due to the high-pressure rise rates [17]. The ignition dwell is positive in RCCI to enhance charge homogeneity through premixing, which minimizes soot formation. Lower in-cylinder temperature is maintained, thus eliminating NO_x formation zones. RCCI utilizes dual fuel premixed combustion to overcome the restrictions of load range by mixing two fuels of distinct reactivity to accomplish reactivity stratification. [18]. The reactivity stratification in RCCI is achieved with port injection (PFI) of high volatile and low reactivity fuel during the

1
2
3 intake stroke and early direct injection (DI) of low volatile and high reactivity fuel during the
4 compression stroke. The combustion advances gradually from the high to low reactivity zones,
5 preventing the high rate of pressure rise and allowing for an extensive load range and improved
6 thermal efficiency [19]. The fuel molecular composition and chemical kinetics influence the
7 start of ignition, combustion duration, operability limit, and formation of emissions in RCCI
8 [20].
9

10 Numerous studies have been conducted on RCCI using standard fuels like gasoline as PFI and
11 diesel as DI fuel [16–18,21,22]. Although RCCI produces high thermal efficiency with lower
12 exhaust emissions than conventional diesel combustion, low-load operations result in higher
13 unburned emissions. Since RCCI uses two different fuels, considerable efforts have been made
14 with various alternative fuels to overcome its limitations [23–25]. Common alternatives to
15 gasoline include methanol, butanol, ethanol, and natural gas, that has been used as low-reactive
16 fuel substitutes [24–27]. Similarly, to replace high reactive fuel, biodiesel, blends of biodiesel
17 with diesel as well as gasoline blended with a cetane improver additive are investigated [27–
18 29]. The lower reactivity gradients between ethanol and diesel as LRF and HRF fuels
19 significantly reduced unburned emissions. [23]. An experiment employing a dual-fuel
20 approach of ethanol and dimethyl ether (DME) found that increasing the ethanol proportion
21 lowered emissions of NO_x and moderately decreased unburned emissions [24].
22
23

24 Three distinct methanol injection strategies were tested in a heavy-duty engine using methanol
25 as LRF in dual-fuel methanol-diesel combustion, wherein methanol port injection reduced
26 unburned emissions more than the direct injection. [26]. The comparative study on RCCI with
27 ethanol and gasoline as low reactive fuels and n-heptane as HRF showed that at high loads,
28 ethanol resulted in increased HC emissions than gasoline but lower NO_x and soot emissions
29 [22]. Experiments on ethanol/biodiesel RCCI revealed higher thermal efficiency, significantly
30 lower NO_x emissions and higher unburned emissions [27]. Another study revealed that n-
31 butanol reduced thermal efficiency and decreased CO emissions. But since n-butanol has a
32 high latent heat of vaporization, HC emission increased [30]. An investigation into the use of
33 different blends of alcohol and gasoline, as well as Karanja biodiesel-diesel blends, as low and
34 high reactive fuels revealed that the butanol-gasoline blend effectively reduced unburned
35 emissions while also achieving better thermal efficiency [29]. At high loads, using 2-butanol
36 and diesel as an LRF and HRF with different premixed ratios resulted in a 7% increment in
37 BTE while simultaneously minimizing NO_x and PM emissions [31].
38
39

40 Biodiesel and polyoxymethylene dimethyl ethers (PODE) are the most widely investigated
41 high-reactivity fuels in RCCI [32,33]. Experiments on gasoline/DME RCCI combustion
42
43
44
45
46
47
48
49
50
51
52
53
54
55
56
57
58
59
60

1
2
3 produced much lower NO_x emissions and somewhat increased HC emissions because of
4 incomplete combustion [32]. Studies on RCCI employing methanol as LRF and PODE as HRF
5 revealed that the higher reactivity of PODE resulted in advanced combustion with reduced
6 combustion duration and elevated NO_x values than methanol/diesel RCCI. The fuel-bound
7 oxygen in PODE helped in minimizing unburned emissions [33]. Pushpak et al. [34]
8 investigated gasoline-methanol and Karanja biodiesel-diesel blends as LRF and HRF,
9 respectively, that improved thermal efficiency and decreased HC emissions than gasoline-
10 diesel. Hanson et al. investigated the effect of injection strategies on RCCI mode at low loads.
11 Using a single fuel strategy, they achieved a 44% ITE at a 2 bar IMEP [35]. An experimental
12 investigation of RCCI under part load conditions was conducted by Wang et al. [36]. They
13 found that the high reactive fuel needs to be significantly increased to expand the low load
14 range. This would improve the overall charge reactivity, which helps to extend the engine
15 operation to low loads.

16 From the literature survey, it is evident that the way the fuel is introduced into the combustion
17 chamber and the fuel reactivity strongly influences the combustion and emission formation in
18 RCCI. Besides, optimizing fuel injection strategies improve thermal efficiency under low-load
19 conditions. Although prior studies explored the impact of alternative fuels on RCCI, the
20 application of fuels derived from waste resources in neat form is yet to be investigated. The
21 present study examines the effects of utilizing plastic waste oil (WPO) and waste cooking oil
22 biodiesel (WCO) as LRF and HRF, respectively, in RCCI. A novel dual fuel port-injected
23 RCCI (PI-RCCI) is investigated to reduce high unburned emissions under low load conditions
24 in RCCI. In PI-RCCI, WPO and WCO are used as LRF and HRF, respectively. The findings
25 of PI-RCCI are compared with the results obtained from WPO/WCO RCCI to examine the
26 improvement in engine performance and reduction in unburned emissions.

26 27 28 29 30 31 32 33 34 35 36 37 38 39 40 41 42 43 44 45 46 47 48 49 50 51 52 53 54 55 56 57 58 59 60

2. Engine Test Setup

The experimental trials were done on a light-duty, single-cylinder diesel engine extensively
utilized for agricultural irrigation pumps (refer to Fig. 1). The essential specification parameters
of the test engine are provided in Table 1. To function in RCCI and PI-RCCI combustion
modes, the intake manifold is modified with a provision for low-pressure and high-pressure
injectors. The existing mechanical direct injection system is also modified into a flexible
common rail high-pressure injection system. A schematic layout of RCCI and PI-RCCI is
shown in Fig. 2.

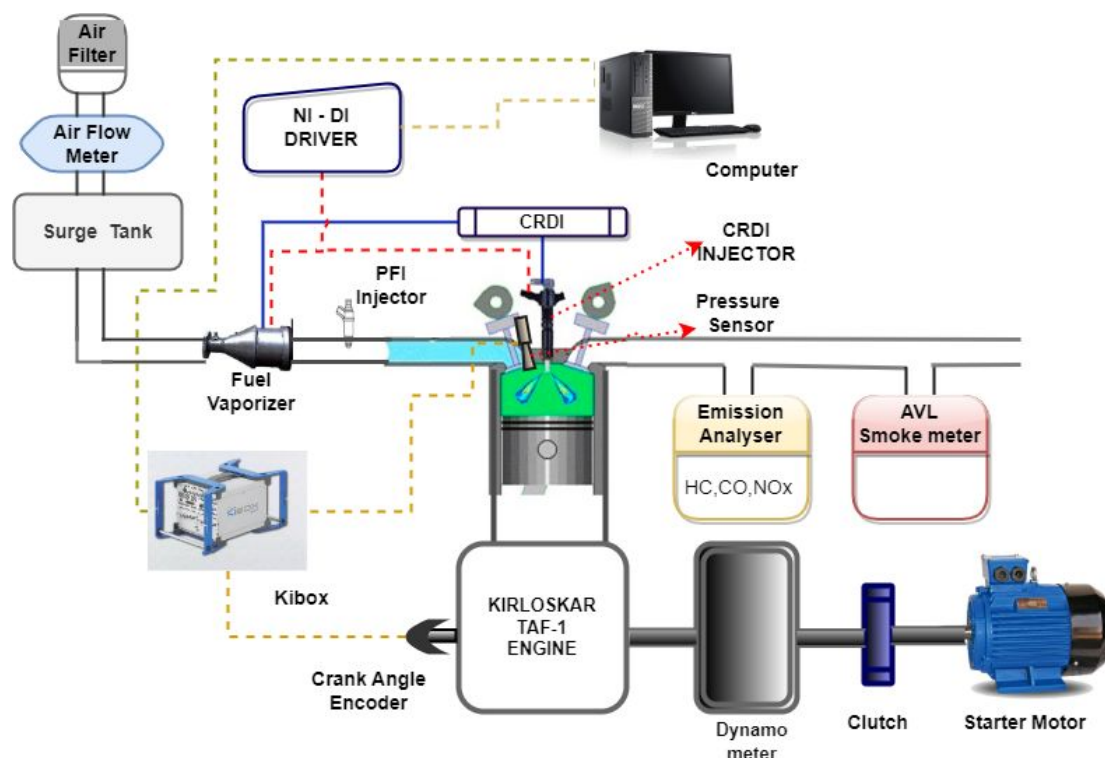


Figure 1 Schematic layout of the test engine setup

Table 1 Experimental engine specifications

Engine type	Air-cooled, naturally aspirated, light duty
Number of Cylinders	Single-cylinder
Rated Power and Speed	4.4 kW at 1500 rpm
Displacement Volume (cc)	662
Cylinder Dimensions (mm)	Cylinder bore 87.5, stroke length 110
Engine Compression ratio	15:1
Fuel Injection Systems	PFI and CRDI
Direct-injected Fuel Pressure (bar)	300
Port-injected Fuel Pressure (bar)	3

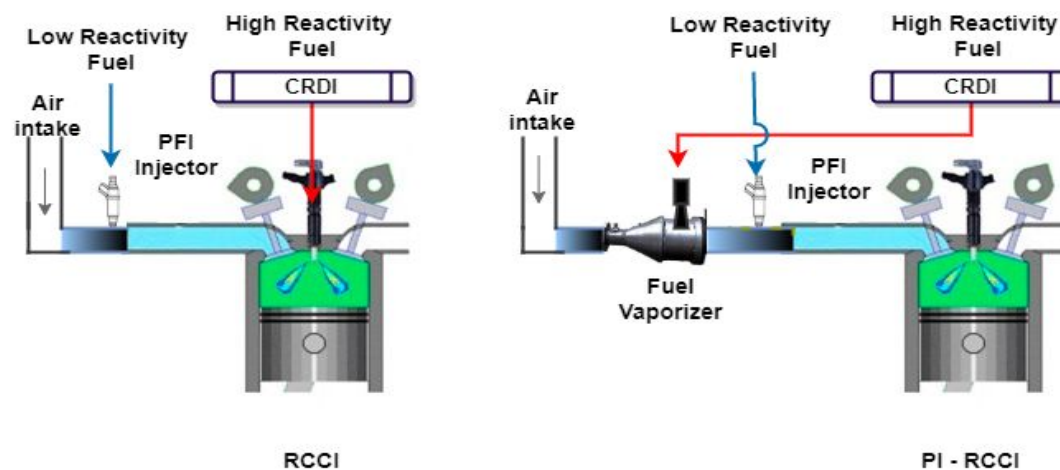


Figure 2 Schematic representation of RCCI and PI-RCCI

1
2
3 A low-pressure PFI injector is mounted on the intake manifold operated by solenoid control
4 for injecting highly volatile fuels. The National Instruments PFI driver adequately controls the
5 timing and duration of port-injected fuel. For implementing RCCI, a flexible DI system is
6 required, for which a common rail fuel injection system has been installed in the cylinder head
7 to provide a fuel injection pressure to the extent of 2000 bar. The CRDI system comprises a
8 fuel injection pump that pressurizes the fuel, a rail that acts as a reservoir and distributes the
9 fuel to the different solenoid injectors, and an injector. Additionally, the CRDI system includes
10 a National Instruments direct injection (DI) driver module that controls the timing and duration
11 of injection. The DI driver also regulates the amplitude of fuel pressure in the rail and the
12 number of injections. A cone-type aluminium fuel vaporizer is installed on the intake manifold
13 to vaporize port-injected high-reactive and low-volatile fuels. A band-type heater is used to
14 heat the entire surface of the fuel vaporizer, and a PID controller controls its surface
15 temperature. WCO is dispersed uniformly at a high injection pressure of 300 bar on the surface
16 of the aluminium vaporizer through a DI injector for achieving PI-RCCI. The constant speed
17 tests at the engine's rated speed are performed using an eddy current dynamometer coupled
18 with the engine flywheel via a cordon shaft. The heat dissipated from the dynamometer is
19 absorbed by circulating cooling water free of ferrous particles. A magnetic filter is employed
20 before it is circulated through the centrifugal pump and into the dynamometer.
21
22
23
24
25
26
27
28
29
30
31
32
33
34
35

36 Table 2 Specifications of measuring instruments

Instrument	Measured Parameter	Range	Accuracy
FID Analyzer	HC	0-10000 ppm	± 10 ppm
NDIR Analyzer	CO	0-10 %	± 0.2 %
Chemiluminescence Analyzer	NO _x	0-10000 ppm	± 5 ppm
Smoke Meter	soot	0-10 FSN	0.001
K-type Thermometer	Temperature	0-1000 °C	± 4 °C
Weighing Bridge	Fuel Mass Flow	0-6 kg	± 0.2 g
Air Flow Meter	Air Flow Rate	1-65 m ³ /h	± 1%

37
38
39
40
41
42
43
44
45
46
47
48
49
50
51 The intake system comprises a surge tank to dampen intake airflow fluctuations and a turbine-
52 type meter to measure the volumetric flow rate of air entering the cylinder. The fuel flow rate
53 is measured using a high-precision weighing bridge. The continuous crank angle and TDC
54 signals are sent to the DI driver module that regulates the timing and duration of fuel injection.
55 The combustion analyzer receives data from the in-cylinder piezoelectric gas pressure sensor
56 and the TDC reference signal from an inductive-type sensor. To determine the apparent net
57
58
59
60

1
2
3 heat release rates, the combustion analyzer processes an average of 100-cycle in-cylinder
4 pressure data and applies the first law of thermodynamics. The total hydrocarbon emissions
5 from the engine are measured using the flame ionization detector (FID). The specifications of
6 other measuring devices are presented in Table 2.
7
8
9

10 The present study intends to understand the effects of using waste resource-based fuels, such
11 as WCO and WPO in RCCI, at varying load settings at a rated speed of 1500 rpm. Also, a novel
12 dual fuel port injected RCCI (PI- RCCI) combustion mode was proposed to mitigate higher
13 unburned emissions in RCCI at low loads. The PI-RCCI involved injecting fuels with varying
14 reactivity into the intake manifold through high and low-pressure injection systems. To provide
15 a baseline, conventional gasoline and diesel were utilized as the port and direct-injected fuels
16 during the experiments. To maximize thermal efficiency, the injection timing of DI fuel and
17 the premixed energy ratio of PFI fuel in RCCI is optimized within a stable combustion regime
18 between a misfire and knocking. The DI timing was varied from 25 CAD bTDC (before top
19 dead centre) in 5 CAD (crank angle degree) intervals up to 40 CAD bTDC for all load settings.
20 The injection timing of PFI fuel was kept constant at 355 CAD bTDC. The premixed energy
21 ratio represents the fraction of port-injected fuel energy to the total energy of PFI and DI fuels
22 in an engine cycle. In PI-RCCI, the ratio of high reactivity fuel energy to the total fuel energy
23 is optimized at each load condition to achieve maximum thermal efficiency.
24
25
26
27
28
29
30
31
32
33
34
35

36 **3. Test Fuel Characteristics**

37 The raw waste cooking oil (WCO) used in the present work was obtained from a local
38 commercial shop that has been filtered and used for extracting waste cooking oil biodiesel.
39 Initially, the free fatty acid (FFA) proportion of raw oil was measured using titration, which
40 was < 2%. The raw oil was converted into biodiesel using a single-step transesterification
41 method due to the low FFA content [34]. The fatty acid methyl ester (FAME) content of
42 biodiesel was measured using a Nucon gas chromatograph equipped with a flame ionization
43 detector, presented in Table 3. The plastic waste segregated from municipal solid wastes is
44 used to extract oil. Municipal plastic waste primarily consists of high-density and low-density
45 polyethylene, polyvinyl chloride and polyethylene terephthalate. Extracting oil from plastic
46 waste involves the pyrolysis process, wherein it is heated to temperatures between 500-550°C.
47 An Agilent make gas chromatograph was used with an Agilent mass spectrometer to measure
48 the plastic waste oil composition. Figure 3 shows the measured composition of the plastic waste
49 oil (WPO). WPO contains many different peaks corresponding to a diverse group of
50
51
52
53
54
55
56
57
58
59
60

hydrocarbons, among which benzene-propyl, 1-ethyl-3-methyl and mesitylene are present in significant fractions commonly found in gasoline.

Table 3 Measured composition of WCO biodiesel [34,35]

FAME type	Palmitic	Stearic	Oleic	Linoleic	Arachidic	Lignoseric
Molecular Formula	$C_{17}H_{34}O_2$	$C_{19}H_{38}O_2$	$C_{19}H_{36}O_2$	$C_{19}H_{34}O_2$	$C_{21}H_{42}O_2$	$C_{25}H_{50}O_2$
Mass (%)	7.85	3.6	33	55	0.66	0.23

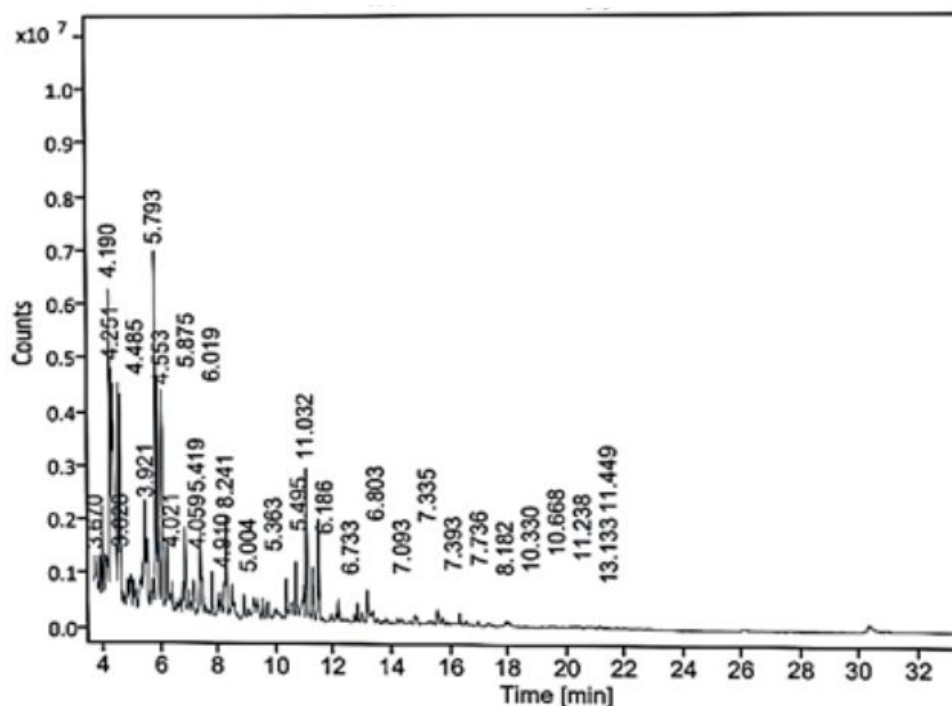


Figure 3 GC-MS profile of plastic waste oil

The kinematic viscosity and density of the test fuels were measured using a rotational viscometer and oscillatory U-tube. The net calorific value was measured using a bomb calorimeter. The measured properties of test fuels are provided in Table 4. The viscosity and density of WPO are comparable to those of gasoline. However, the calorific value of WPO is lower compared to gasoline. The WCO has a higher viscosity than diesel, with a lower calorific value. However, it had a higher cetane rating and density than diesel. Based on the fuel characterization, WPO and WCO are chosen as LRF and HRF, respectively, for RCCI and PI-RCCI.

Table 4 Test fuel properties [35]

Properties/Fuels	Gasoline	WPO	Diesel	WCO Biodiesel
Net calorific value (MJ/kg)	42.68	42.62	44.32	39.6
Cetane number	-	-	47	>51
Octane number	91	-	-	-
Density @ 20°C (kg/m ³)	717	765	814	826
Viscosity @ 20°C (mm ² /s)	--	0.56	2.82	7.34
Flashpoint (°C)	- 43	12	55	178

4. Results and Discussion

The findings of the present study are presented in two sections. The first section compares the results obtained using WPO/WCO RCCI with the baseline RCCI that uses gasoline as the port-injected fuel and diesel as the direct-injected fuel (G/D RCCI). The results of the dual fuel port injection RCCI strategy with WPO and WCO as LRF and HRF are then discussed to examine the potential for reducing high unburned emissions in RCCI.

4.1. Comparison of G/D RCCI with WPO/WCO RCCI

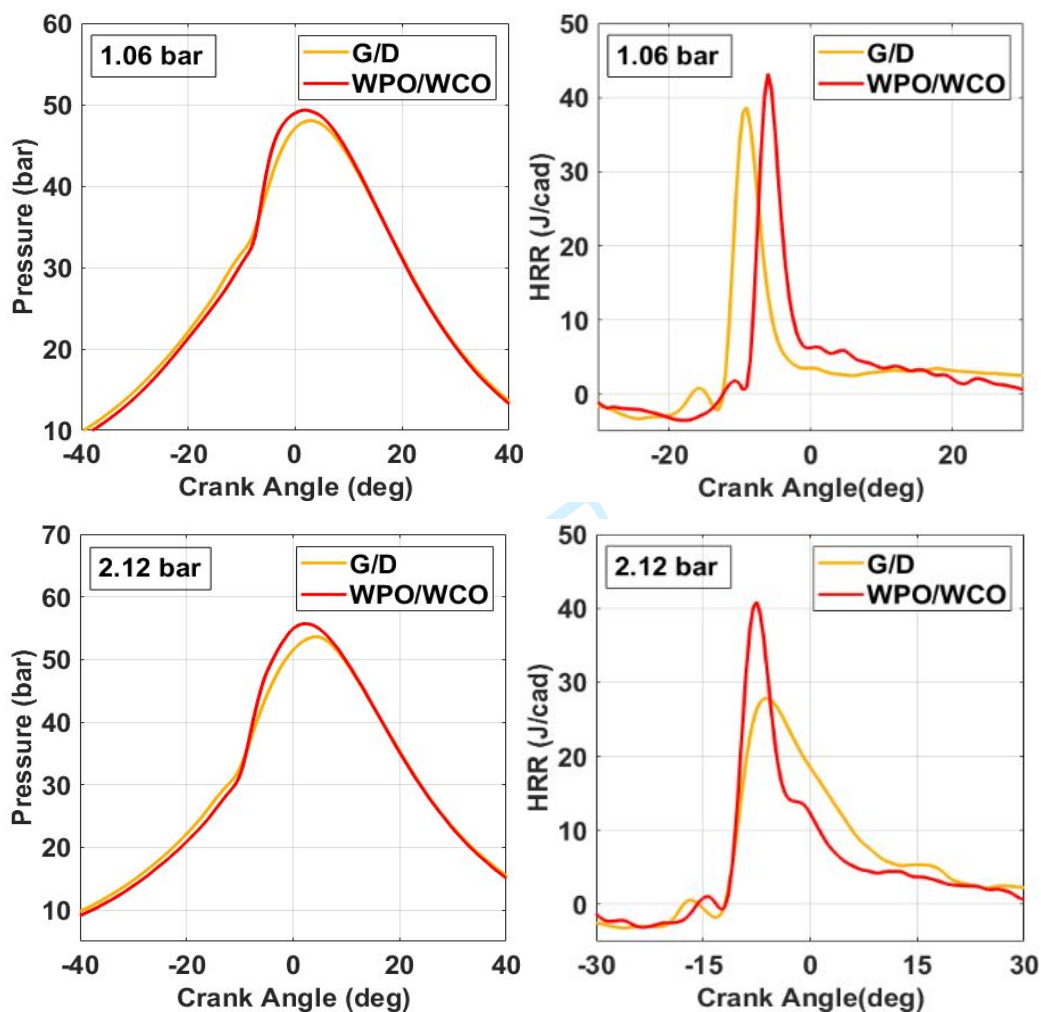
The experiments were conducted under similar operating conditions to evaluate the combustion and performance of WPO/WCO RCCI compared to the baseline RCCI operated with gasoline and diesel. The results obtained under optimized operating conditions with WPO/WCO RCCI are compared with G/D RCCI. The optimum start of injection (SOI) timing of DI fuel results in better combustion phasing, which corresponds to maximum brake thermal efficiency (BTE). At the same SOI, increasing the premixed energy ratio (PER) more than the optimum value resulted in high unburned emissions, and the combustion entered a misfire region at very high PER values. A detailed discussion on the parametric study of the effects of SOI and PER on G/D RCCI is available in Pandian and Anand [18]. The DI timings and PER in WPO/WCO RCCI have similar effects as in G/D RCCI. Table 5 provides the optimized parameters corresponding to achieving maximum BTE for both fuel combinations in RCCI.

Table 5 Operating conditions and optimized parameters for RCCI

Parameters		Optimized Values			
BMEP (bar) / Rated load (%)		1.06 / 20	2.12 / 40	3.19 / 60	4.24 / 80
Premixed energy ratio (%)	G/D	39	61	81	93
	WPO/WCO	28	54	86	96
SOI timing of DI fuel (CAD bTDC)	G/D	30	30	30	30
	WPO/WCO	25	30	30	30

4.1.1. Combustion Characteristics

The pressure and heat release rate profiles of G/D and WPO/WCO RCCI at different loads are presented in Figure 4. WPO/WCO RCCI results in an earlier ignition, a higher rate of heat release and peak pressure than G/D RCCI across all loads. The use of WCO biodiesel as HRF, which has a higher cetane rating than diesel, increases the reactivity of the direct-injected fuel. Thus, the ignition delay was reduced with an early ignition in the case of WPO/WCO RCCI compared to diesel as HRF in G/D RCCI.



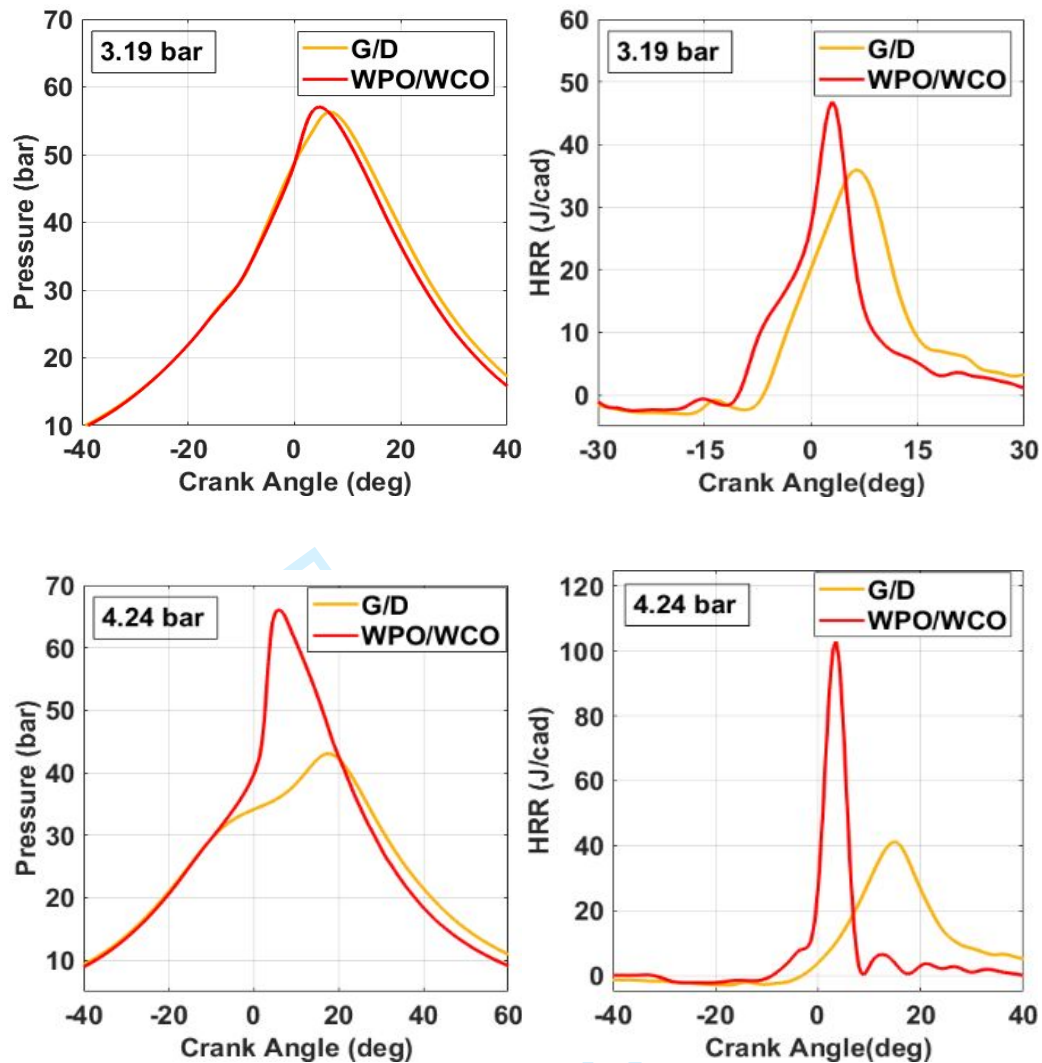


Figure 4 Comparison of pressure and heat release rate profiles of G/D and WPO/WCO RCCI.

A two-stage heat release is a defining characteristic of RCCI combustion and is observed in both G/D and WPO/WCO RCCI at all load conditions. In RCCI, a low-temperature heat release (LTHR) is caused by the high reactivity fuel having a lower ignition temperature, followed by the heat release of premixed charge. The waste cooking oil with a high cetane number increases the in-cylinder charge reactivity and initiates early flame oxidation reactions before the high-temperature heat release (HTHR). In WPO/WCO RCCI for similar DI timings, the LTHR occurs earlier than in the G/D RCCI due to the increased charge reactivity. As a result, the combustion of the premixed charge starts immediately after the LTHR with a reduced time lag between the high-temperature heat release and LTHR. With load increment, the optimum PER increases in WPO/WCO RCCI, decreasing the magnitude of LTHR. The maximum pressure and heat release rate occur earlier in WPO/WCO RCCI. As the load increases, the low-reactivity fuel proportion is increased to prevent knocking combustion caused by the injection

of high-reactivity fuel during the compression stroke. Given the increasing proportion of low-reactivity fuel with higher loads, the peak pressure is delayed and shifts further away from TDC. Due to the early initiation of ignition and advanced combustion phasing in WPO/WCO, maximum pressure and heat release occurred closer to TDC.

The duration and phasing of combustion for WPO/WCO RCCI are compared to that of G/D RCCI at various load conditions in Figure 5. The combustion duration is estimated as the crank angle between the start and end of combustion, defined as 5% and 90% of total heat release, respectively. The combustion phasing is defined as the crank angle instant wherein 50% of cumulative heat is released. With alternative fuels, the increased reactivity of WCO fuel initiates combustion early with an early phasing and reduced duration. Except at 1.06 bar BMEP, the combustion phasing is significantly more advanced with WPO/WCO than G/D. With similar SOI timings of DI fuel in G/D and WPO/WCO, the high reactivity of the charge with WCO resulted in early ignition and advanced combustion phasing. As discussed earlier, it also increases pressure rise and heat release rate with WPO/WCO RCCI. The slightly retarded timing of DI fuel with WPO/WCO at 1.06 bar BMEP resulted in comparable combustion phasing to G/D RCCI. The combustion duration is reduced with WPO/WCO RCCI at all loads compared to G/D RCCI. The cumulative effects of increased reactivity of in-cylinder mixture, higher burn rate and optimal combustion phasing resulted in a shorter combustion duration with WPO/WCO RCCI than G/D.

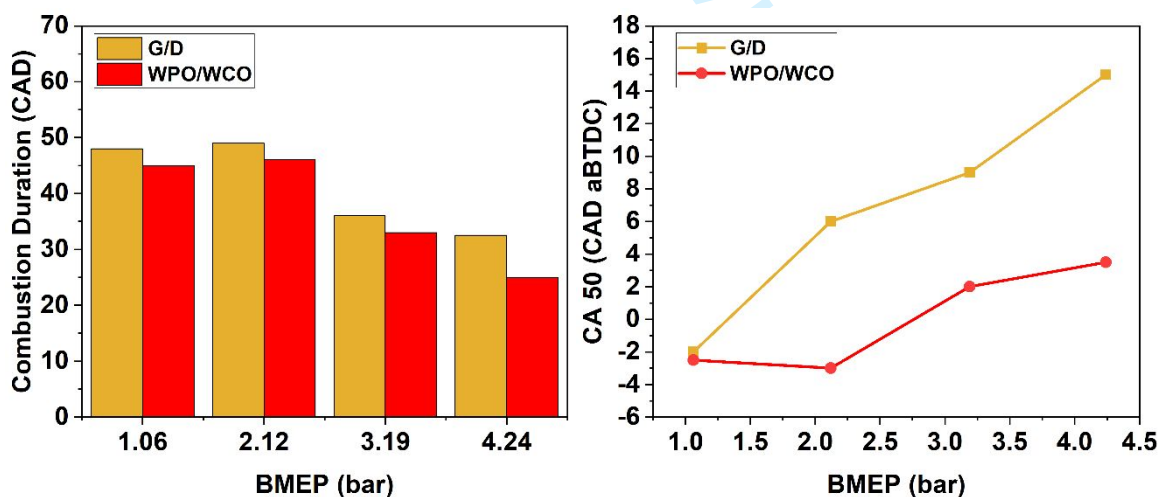


Figure 5 Comparison of combustion duration and combustion phasing at varying loads in G/D and WPO/WCO RCCI

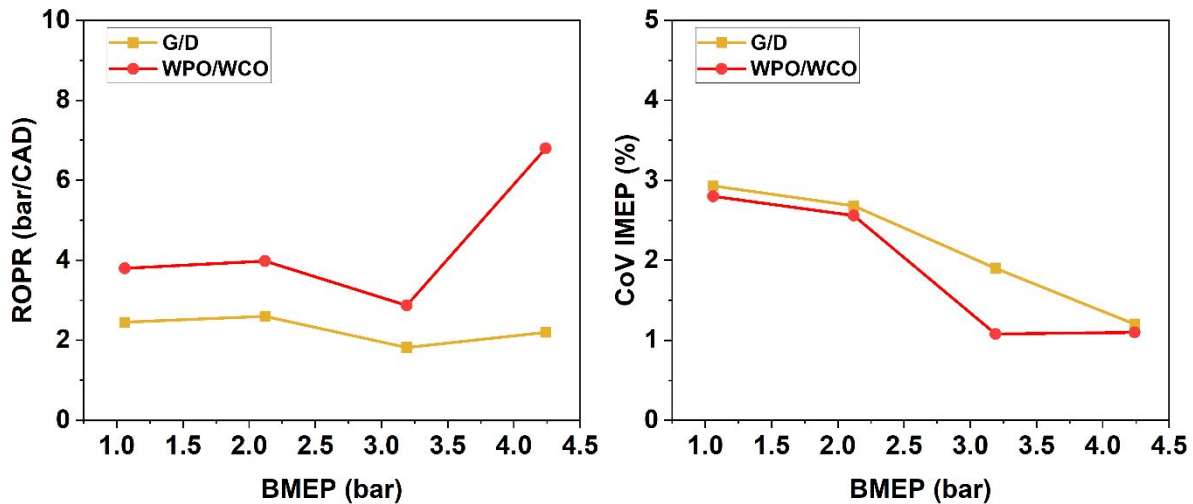


Figure 6 Comparison of ROPR and CoV_{IMEP} at varying loads in G/D and WPO/WCO RCCI

The rate of pressure rise (ROPR) and coefficient of variation in IMEP (CoV_{IMEP}) with G/D and WPO/WCO RCCI at varying load conditions are shown in Fig. 6. WPO/WCO RCCI resulted in higher pressure rise rate at all loads than G/D. Advanced ignition timing and increased heat release rate in WPO/WCO lead to a higher rate of pressure rise than G/D. The retarded peak pressure, combustion duration and its occurrence during the expansion stroke resulted in a reduced pressure rise rate in G/D than WPO/WCO. CoV_{IMEP} is well within the misfire limit for both G/D and WPO/WCO RCCI. At higher load conditions, in-cylinder temperature increases, reducing the misfiring tendency and resulting in a lower CoV_{IMEP} with both fuels.

4.1.2. Engine Performance Characteristics

The engine brake thermal efficiency (BTE) and brake specific fuel consumption (BSFC) with G/D and WPO/WCO RCCI are presented in Figure 7. WPO/WCO RCCI resulted in higher BTE than G/D at all load conditions. In WPO/WCO RCCI, the occurrence of peak pressure near the top dead centre (TDC) with a higher magnitude improves positive displacement work. The cumulative effects of higher peak pressure, optimal combustion phasing and enhanced combustion owing to fuel-bound oxygen of WCO biodiesel increased BTE. A maximum increase in BTE of 29% is obtained at 2.12 bar BMEP with WPO/WCO RCCI than G/D RCCI. Similarly, BSFC values in WPO/WCO RCCI were lower than G/D at all the loads. Lower unburned hydrocarbon emissions discussed later indicate complete combustion in WPO/WCO RCCI, contributing to reduced BSFC and higher BTE with WPO/WCO than G/D.

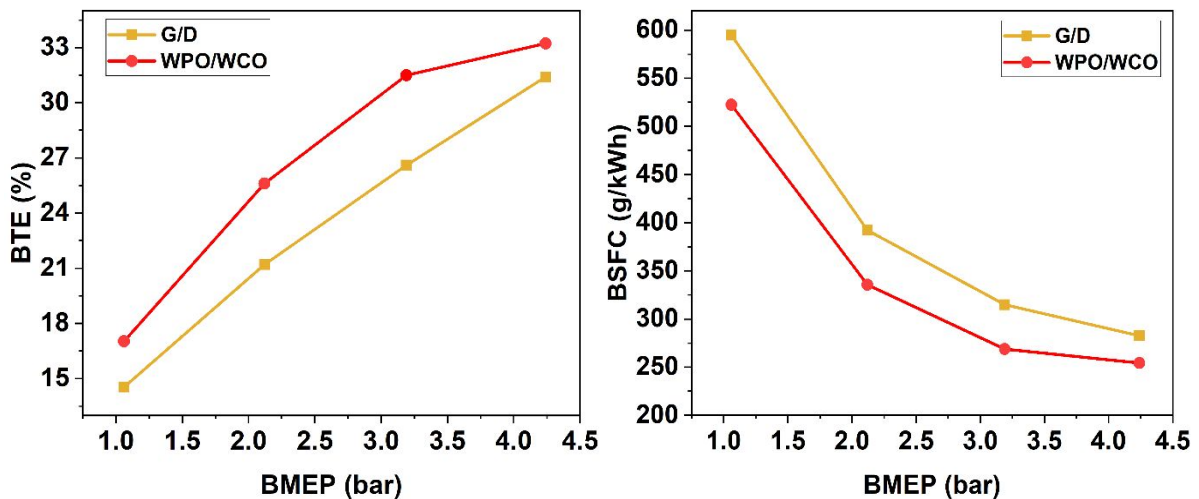


Figure 7 Comparison of BTE and BSFC at varying loads in G/D and WPO/WCO RCCI

4.1.3. Engine Exhaust Emissions

The unburned hydrocarbon (HC) and carbon monoxide (CO) emissions at different load conditions with WPO/WCO and G/D RCCI are shown in Figure 8. It has been well documented in the literature that LTC combustion modes, such as RCCI, tend to produce higher levels of unburned emissions due to reduced in-cylinder temperatures, oxidation rates and increased crevice flow of premixed charge. RCCI results in significantly high HC and CO emissions, especially at part load conditions. The high combustion temperature, advanced combustion phasing, and fuel-bound oxygen in WCO enhanced the combustion and oxidation rates, resulting in reduced HC and CO emissions in WPO/WCO than G/D RCCI. Because of the improved conditions inside the cylinder for oxidation and combustion, CO and HC emissions have decreased significantly at higher loads. A maximum reduction in CO and HC emissions of up to 36% and 50%, respectively, at 1.06 bar BMEP obtained with WPO/WCO than G/D RCCI.

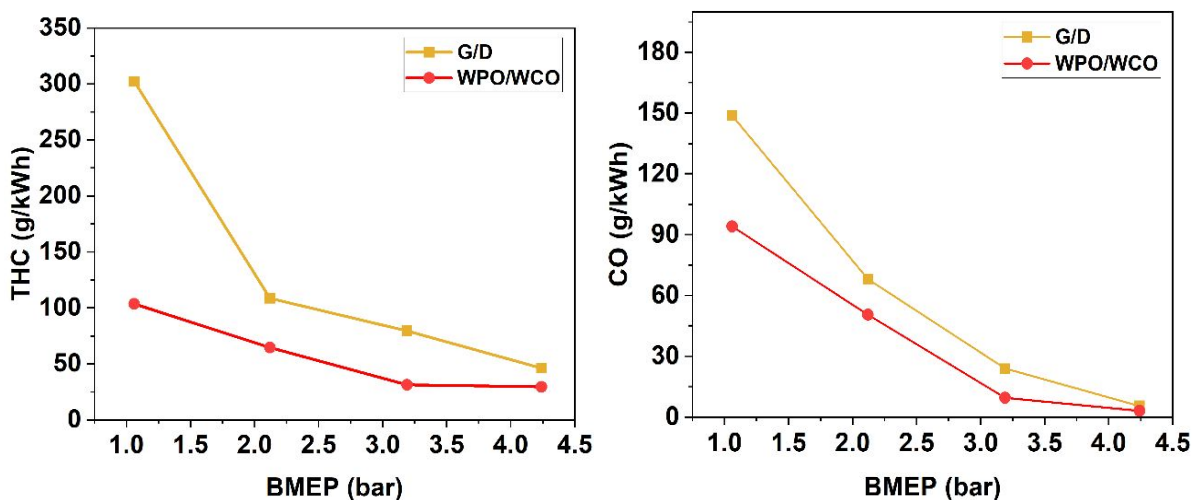


Figure 8 Variations in HC and CO emissions at varying loads in G/D and WPO/WCO RCCI

The NO_x and soot emissions variations in G/D and WPO/WCO RCCI under varying loads are shown in Fig. 9. NO_x emissions are higher for WPO/WCO than G/D at all load conditions due to the higher combustion temperature, advanced combustion phasing and fuel-bound oxygen of WCO biodiesel. At higher loads, the reduction in total reactivity of the charge within the cylinder due to increased premixed energy share leads to a delay in combustion phasing, resulting in a shorter residence time for NO formation kinetics. This results in lower NO_x emissions for both G/D and WPO/WCO. It is well known that RCCI is a premixed homogenous combustion that results in an ultra-low soot formation. The results obtained with G/D and WPO/WCO RCCI confirm the same. With both G/D and WPO/WCO, the smoke emissions are less than 0.01 FSN.

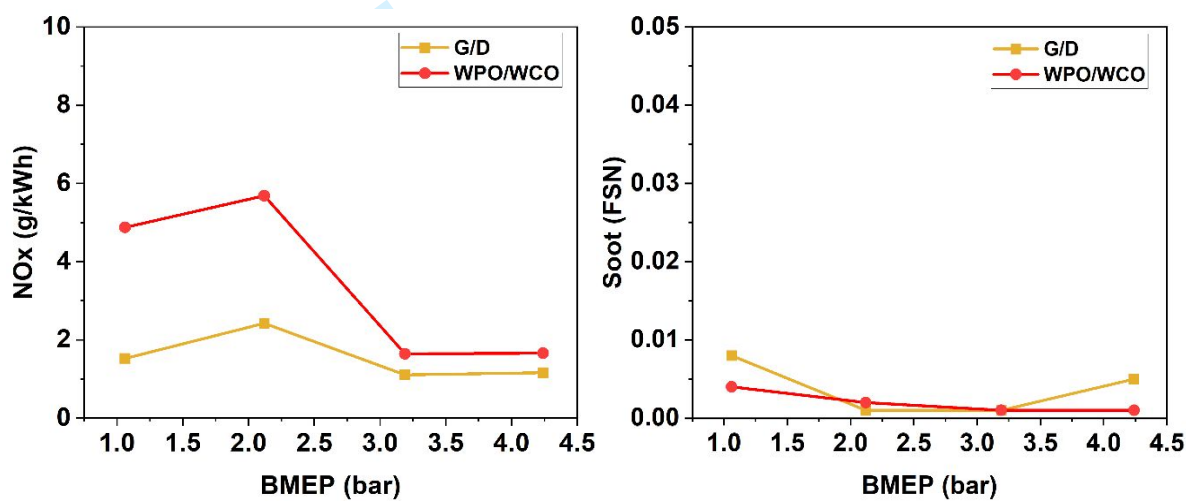


Figure 9 NO_x and soot emissions variations with load for G/D and WPO/WCO RCCI

4.2 PI-RCCI with Alternative Fuels

RCCI operation with alternative fuels, WPO/WCO, effectively decreased the unburned emissions, but NO_x emissions slightly increased. Utilizing high-reactivity fuel through port injection is studied to reduce unburned emissions at low load conditions further. In PI-RCCI, the low and high-reactivity fuels are injected into the intake manifold during the intake stroke. Plastic waste oil and waste cooking oil are used as low (LRF) and high reactivity fuel (HRF), respectively. WPO is injected using a low-pressure PFI injector mounted on the intake port in the same way as in the G/D RCCI. A cone-type fuel vaporizer facilitates the vaporization of high reactive and low volatile WCO biodiesel injected into the intake manifold. The WCO biodiesel is injected at 300 bar injection pressure using a high-pressure CRDI injector. The high-pressure WCO biodiesel is injected into the heated inner surface of the fuel vaporizer, which is heated by a circumferential band-type heater. In PI-RCCI, the injection timing and

1
2
3 duration of both LRF and HRF are varied to optimize the combustion process. A premixed
4 mixture is formed inside the cylinder by injecting the LRF and HRF into the intake manifold
5 over the air stream. The reactivity of the fuel-air mixture entering the cylinder can be adjusted
6 by adjusting the proportion of high and low-reactivity fuels, which can help achieve improved
7 combustion and emission reduction.
8
9

10
11 The port injection timing of WPO and WCO is fixed at 355 CAD bTDC. The WPO energy
12 ratio (WPOER) is systematically increased to vary the mixture reactivity inside the engine
13 cylinder. The WCO (HRF) injected into the vaporizer at high pressure vaporizes instantly and
14 is mixed with the WPO (LRF) injected into the intake manifold. Thus, the vaporized fuels have
15 sufficient time to mix with the air resulting in a homogeneous air-fuel mixture before ignition.
16 In PI-RCCI, the injection of HRF fuel through the intake manifold leads to an earlier
17 combustion initiation than in RCCI. As the proportion of high-reactivity fuel decreases with an
18 increase in the WPO ratio, the reactivity of the overall mixture decreases, resulting in a delayed
19 start of combustion.
20
21
22
23
24
25
26
27
28

29 **4.2.1 Effects of Varying WPO energy ratio in PI-RCCI**

30 In PI-RCCI, the desired charge reactivity inside the cylinder can be achieved using different
31 mixing ratios of high reactive WCO and low reactive WPO. The experiments are conducted at
32 a fixed load by varying the WPO proportions in the mixture. The desired engine load is
33 maintained by increasing WPO proportion and decreasing WCO correspondingly. The impact
34 of the WPOER on PI-RCCI combustion is studied, and the results are presented next. WPOER
35 is the ratio of plastic waste oil energy to total fuel energy.
36
37
38
39
40

41 **4.2.2. Combustion Characteristics of PI-RCCI**

42 Figure 10 shows the pressure and HRR profiles of PI-RCCI with an increase in WPO energy
43 ratios at 1.06 bar BMEP load. An early start of combustion is observed in PI-RCCI due to the
44 injection of high reactive WCO into the vaporizer during the intake stroke, which results in an
45 advanced combustion phasing and higher pressure rise rate. The vaporizer is maintained at
46 180°C to aid the vaporization of low volatile WCO, which elevates the charge temperature
47 entering the cylinder. To suppress the self-ignition of WCO, the LRF proportion needs to be
48 increased. The proportion of LRF injected into the cylinder significantly affects the global
49 reactivity. With an increase in the WPOER, there is a delayed start of combustion, and the
50 combustion phasing is shifted towards TDC. As the proportion of LRF (WPO) in PI-RCCI
51 increases, the combustion process shifts from a two-stage heat release to a single-stage heat
52
53
54
55
56
57
58
59
60

release. Also, the combustion phasing becomes more delayed, and a reduction of peak pressure and maximum HRR is observed.

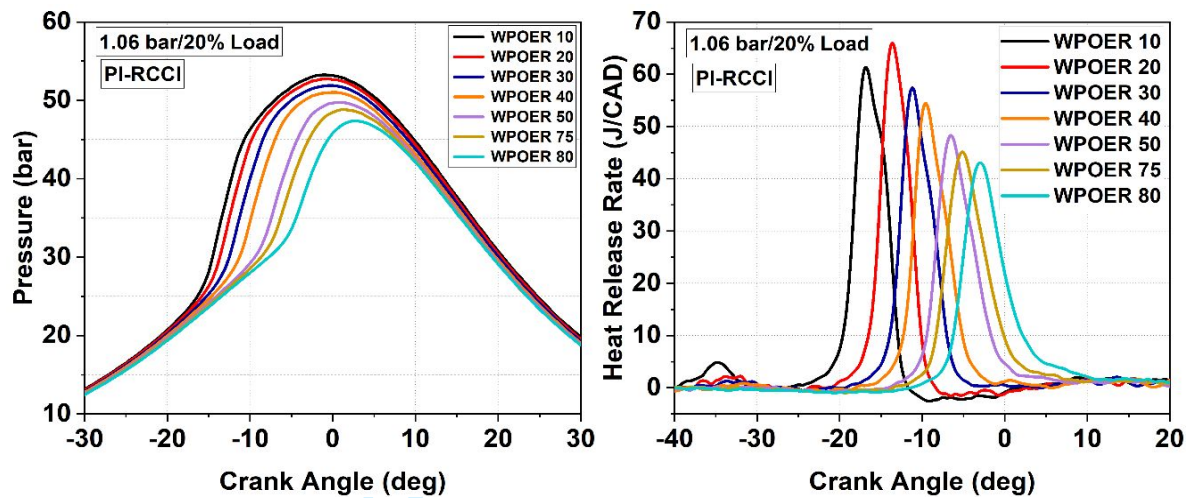


Figure 10 Comparison of pressure and HRR profiles with increasing WPOER at 20% load in PI-RCCI

4.2.3. Engine Performance Characteristics of PI-RCCI

Figure 11 shows the BTE and BSFC variation at 1.06 bar BMEP in PI-RCCI. It shows that as the WPOER increases, the BTE increases gradually. At a lower WPO energy ratio, an advanced combustion phasing and a higher pressure rise rate during the compression stroke increased the negative work. The higher WPO energy ratio reduced the pressure rise rate and improved the combustion phasing, helping to achieve better BTE. The maximum BTE is obtained with a WPOER of 75%. Increasing the WPO quantity further makes combustion unstable and shifts away from TDC. Also, the unburned emissions increased rapidly with very high WPO.

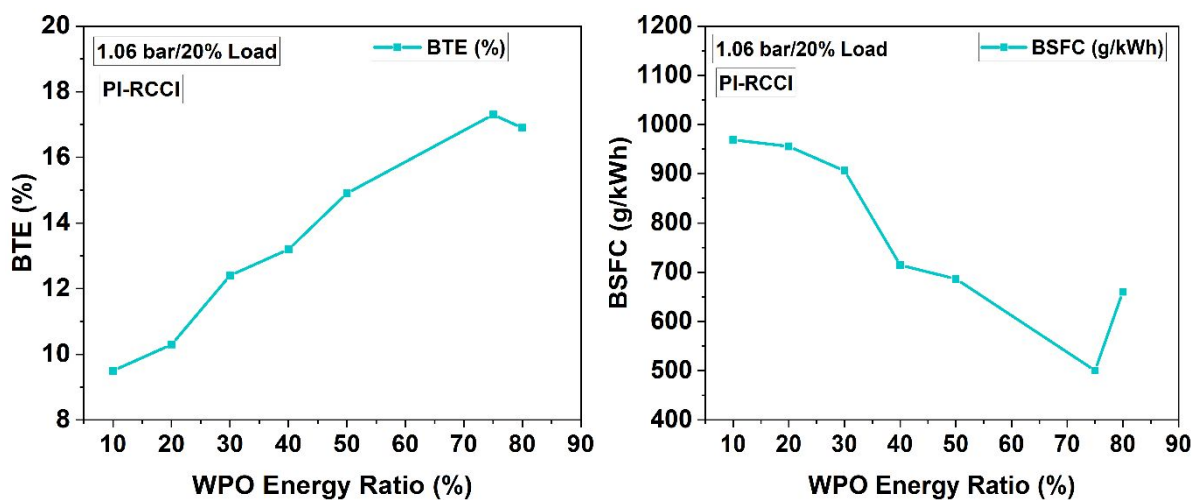


Figure 11 Comparison of BTE and BSFC with varying WPOER at 20% load in PI-RCCI

4.2.4. Emission Characteristics of PI-RCCI

Figure 12 compares HC and CO emissions with varying WPO energy ratios at 1.06 bar BMEP load in PI-RCCI. The unburned emissions have shown a decreasing trend with an increase in the WPO energy ratio. This trend could be due to better air-fuel mixing because of increased ignition delay with high WPO proportion. An increase in WPO ratio above 75% resulted in a steep increment in CO and HC emissions. The obtained results show that changes in overall mixture reactivity and in-cylinder conditions significantly influence unburned emissions.

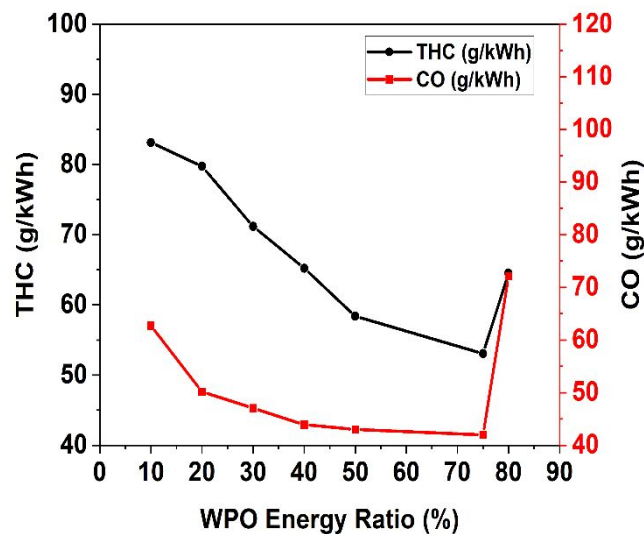


Figure 12 Comparison of HC and CO emissions with varying WPOER at 1.06 bar BMEP load in PI-RCCI

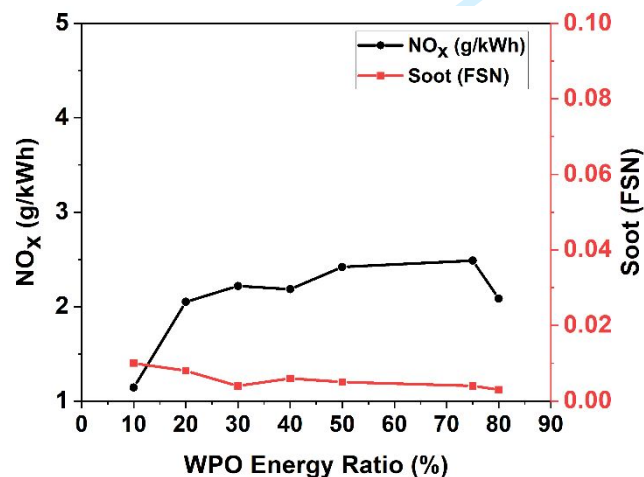


Figure 13 Comparison of NO_x and soot emissions with varying WPOER at 20% load in PI-RCCI

Figure 13 compares NO_x and soot emissions with varying WPOER at 1.06 bar BMEP in PI-RCCI. Premixed lean homogenous mixture combustion in PI-RCCI reduced NO_x emission.

Initially, when the WPO energy ratio is increased from 10 to 20%, the NO_x emissions showed an increasing trend; subsequently, there are no significant changes. The maximum value of NO_x obtained is 2.4 g/kW.hr at 75 % WPOER. Port injection of both fuels provides sufficient time for mixing fuel and air, thus eliminating the soot formation zones. The soot values obtained are well below 0.01 FSN for all different WPOERs. Therefore, the changes in total reactivity in PI-RCCI had no substantial influence on NO_x and soot formation.

It should be noted that the impact of varying WPOER on PI-RCCI combustion and emissions at 1.08 bar BMEP is presented here, wherein the unburned emissions are significantly higher at this condition. The trends obtained at other loads are similar and not shown for brevity.

4.3. Comparison of PI-RCCI and RCCI with Alternative Fuels

The best thermal efficiency is achieved by varying the WPO energy ratio in PI-RCCI. The results obtained in PI-RCCI at optimized operating conditions are compared with RCCI combustion with WPO and WCO as LRF and HRF. The maximum attainable load with PI-RCCI is only up to 40% of the full load due to the high rate of pressure rise and knocking combustion beyond this load condition. Table 6 provides the optimal parameters for RCCI and PI-RCCI to obtain maximum BTE.

Table 6 Optimized parameters at different loads for maximum BTE

Parameters		Optimized values	
BMEP (bar)		1.06	2.12
Rated load (%)		20	40
Plastic waste oil energy ratio (%)	PI-RCCI	75	93
	RCCI	28	54

4.3.1. Combustion Characteristics

The pressure and HRR profiles obtained in PI-RCCI are compared with RCCI at two load conditions in Fig. 14. The pressure profile of PI-RCCI with 75% WPOER is similar to those obtained in RCCI with 28% WPOER. The characteristic LTHR is not present in the case of PI-RCCI because of a high proportion of low-reactivity fuel in the mixture. The higher amount of LRF suppresses the autoignition of WCO shifting the combustion phasing towards compression TDC. The HRF injected through a high-temperature fuel vaporizer increases the intake charge temperature in PI-RCCI, which also increases the temperature of the charge inside the cylinder during compression. Therefore, the high temperature promotes an early start of combustion during the compression stroke resulting in an undesirable pressure rise rate, thus

limiting the achievable load range in PI-RCCI. In PI-RCCI, the combustion process is initiated by injecting high-reactivity fuel during the intake stroke, resulting in a highly premixed air-fuel mixture. This leads to a faster pressure rise and heat release rates than RCCI, where the combustion proceeds progressively from low to high reactivity regions. It can be inferred that, unlike RCCI, the charge stratification of DI fuel is absent in PI-RCCI. At 2.12 bar BMEP, the combustion in PI-RCCI is instantaneous with a high-pressure rise rate limiting the extension of load further. The LRF required to attain a 2.12 bar BMEP is more than 90%. Since the cetane rating of WCO biodiesel is high, an extremely high proportion of LRF is necessary to suppress the early auto-ignition in PI-RCCI. Increasing the load beyond 2.12 bar BMEP, an associated increase in HRF caused premature ignition with a high-pressure rise rate limiting the achievable load range.

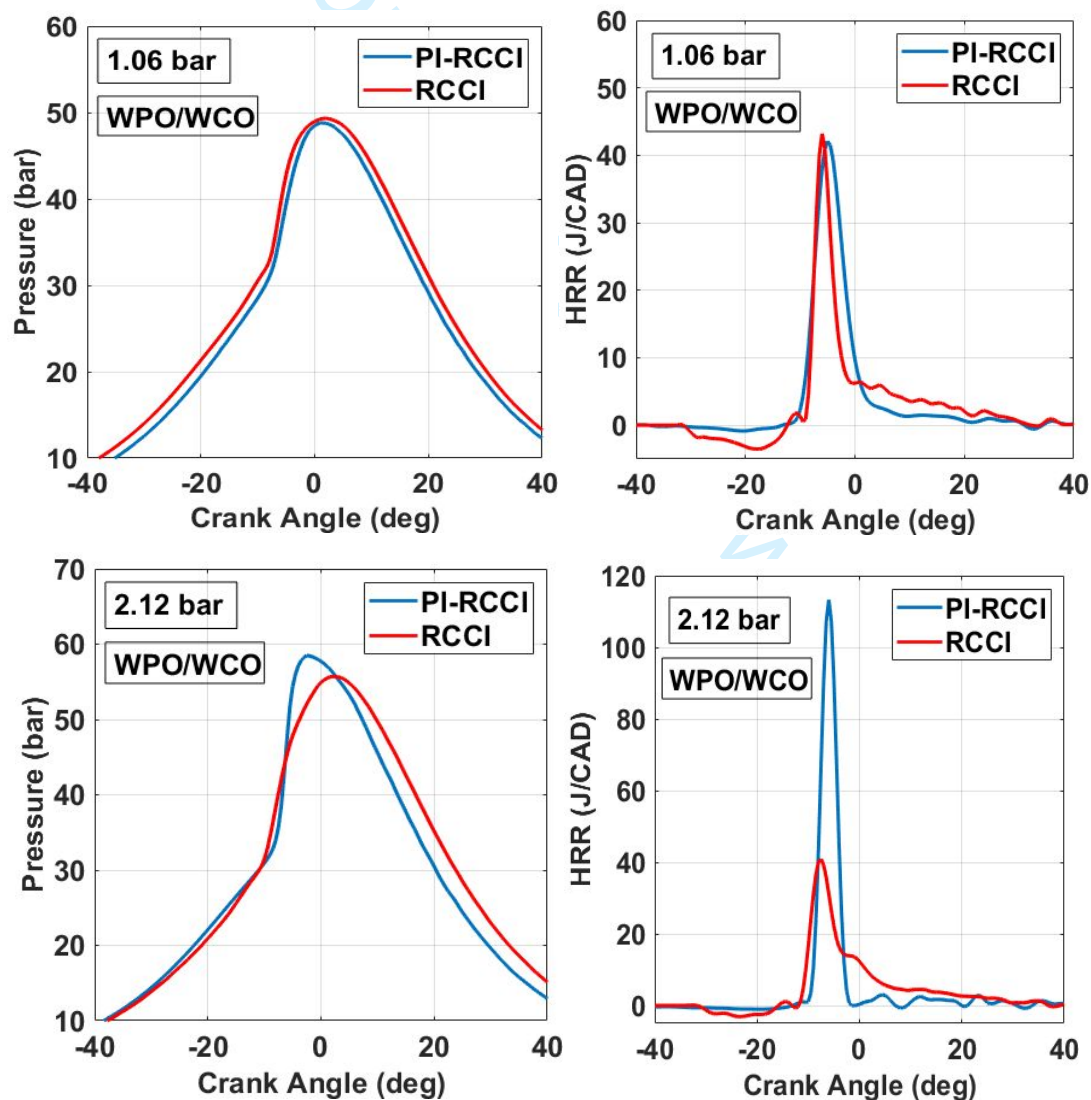


Figure 14 Comparison of pressure and heat release rate profiles of RCCI and PI-RCCI

Figure 15 shows the CoV_{IMEP} and rate of pressure rise (ROPR) at different load conditions with WPO/WCO RCCI and PI-RCCI. The combustion process in PI-RCCI results in higher pressure rise rate than RCCI due to the highly premixed fuel and early combustion phasing. The CoV_{IMEP} was similar and well within the misfire limits for both RCCI and PI-RCCI.

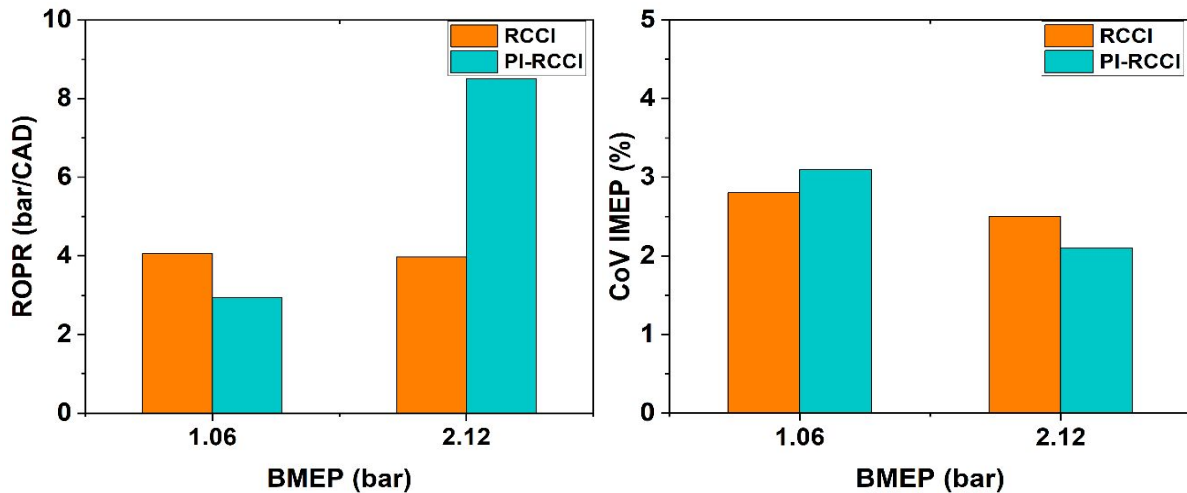


Figure 15 Comparison of rate of pressure rise and CoV_{IMEP} at varying loads in RCCI and PI-RCCI

4.3.2. Engine Performance Characteristics

Figure 16 shows the variations in BTE and WPOER at different load conditions in RCCI and PI-RCCI. It is observed that the BTE in the case of WPO/WCO PI-RCCI is comparable to that of RCCI, while the WPO energy ratio is significantly high.

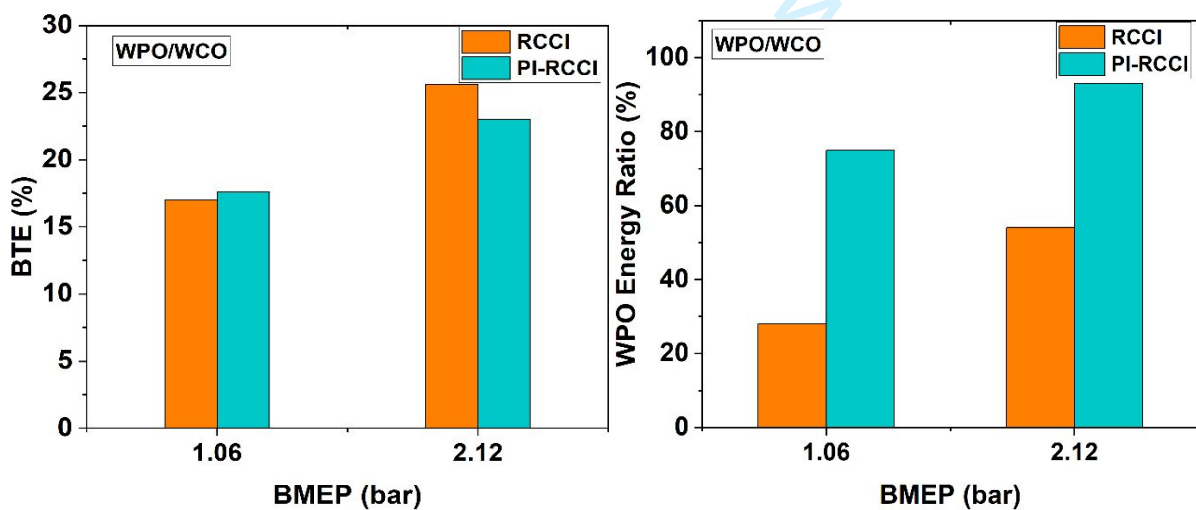


Figure 16 Comparison of BTE and WPO energy ratio at varying loads in RCCI and PI-RCCI

At 1.06 bar BMEP, the BTE is slightly higher with PI-RCCI attributed to highly premixed lean combustion with reduced unburned emissions and higher combustion efficiency. High pressure during the compression stroke increases negative work at a 2.12 bar BMEP load in PI-RCCI, resulting in decreased BTE compared to RCCI. The optimum WPO energy ratio required is considerably increased in the case of PI-RCCI. A higher proportion of low reactivity WPO is required in PI-RCCI to suppress the early autoignition of WCO.

4.3.3. Emission Characteristics

Figure 17 compares the HC and CO emissions trend with WPO/WCO RCCI and PI-RCCI. RCCI investigations have shown that it resulted in higher unburned emissions due to reduced combustion temperature, oxidation rate, and increased crevice flow of premixed charge. The high HC emissions could also be attributed to spray wall wetting of advanced injection timing of high reactivity fuel [36]. The advanced combustion phasing in PI-RCCI, combined with the higher intake charge temperature, improves oxidation rates, reducing HC and CO emissions. In PI-RCCI, the enhanced combustion and oxidation reduced HC emissions by 48% at 1.06 bar BMEP. The higher proportion of high volatile low reactivity fuel in the case of PI-RCCI forms a highly homogeneous mixture. The CO emissions are also reduced in PI-RCCI up to 70% at 40% load compared to RCCI. As the load increases, the CO and HC emissions are reduced in both combustion modes due to higher temperatures and increased oxidation rates.

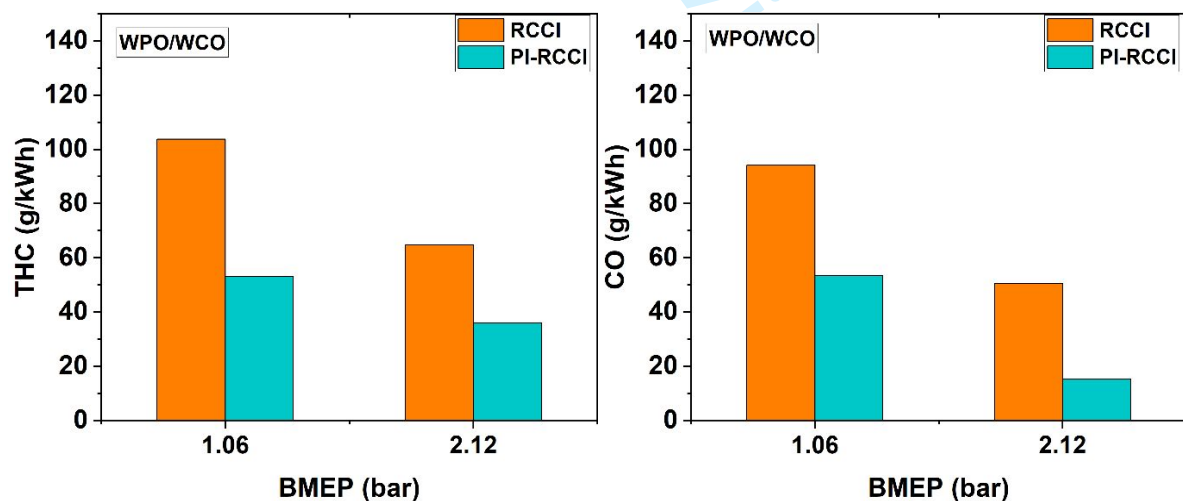


Figure 17 Comparison of HC and CO emissions at varying loads in RCCI and PI-RCCI

Figure 18 compares soot and NO_x emissions in WPO/WCO RCCI and PI-RCCI at varying loads. RCCI combustion results in a low NO_x emission due to a reduced in-cylinder

temperature. In PI-RCCI, the fuel injected early during the combustion cycle provides sufficient time to blend with intake air, thus eliminating fuel-rich zones. Therefore, lean homogenous mixture combustion in PI-RCCI results in lower NO_x values than RCCI. The NO_x values decreased up to 69 % at 2.12 bar BEMP. Soot emissions remained lower than 0.01 FSN in RCCI and PI-RCCI.

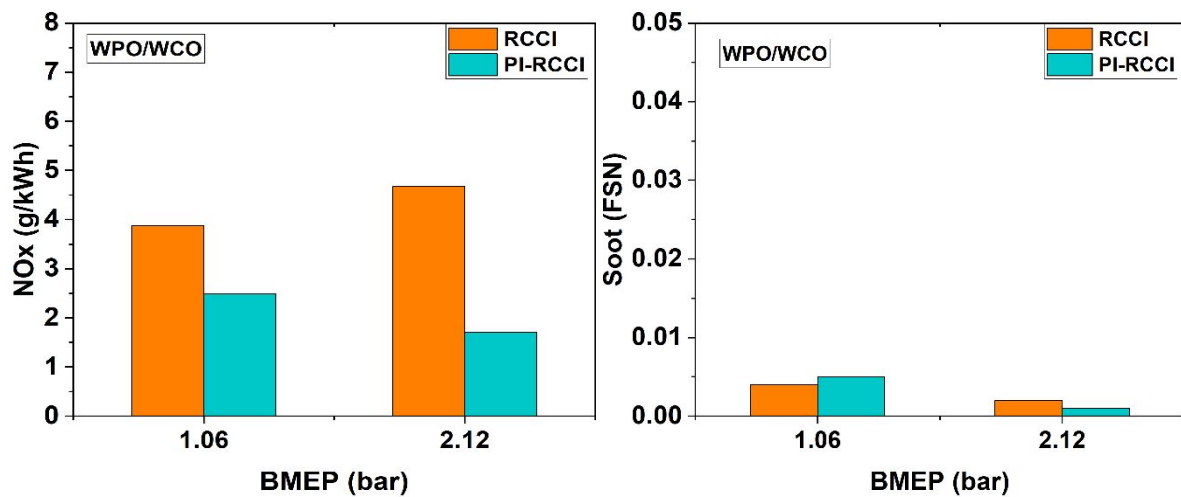


Figure 18 Comparison of NO_x and soot emissions at varying loads in RCCI and PI-RCCI

5. Conclusions

In the present study, experimental investigations are conducted in a modified single-cylinder diesel engine with a custom fuel injection system to test the performance of RCCI and PI-RCCI modes using conventional gasoline-diesel and alternative fuels such as plastic waste oil (WPO) and waste cooking oil (WCO) biodiesel. The DI fuel timings and premixed energy ratio are optimized to achieve maximum BTE in RCCI. A novel PI-RCCI mode was also explored to decrease the high unburned emissions at low loads in RCCI. In PI-RCCI, both low and high-reactivity fuels, viz. WPO and WCO are injected into the intake manifold during the intake stroke. The WPO energy ratio is optimized in PI-RCCI for achieving a maximum BTE, and the effect of the different mixing ratios of WPO with WCO is studied. The major conclusions obtained from the current study are as follows.

- i. WPO/WCO RCCI experiments have shown that alternative fuels extracted from waste resources can be used in neat form, resulting in enhanced engine performance and reduced exhaust emissions compared to G/D RCCI.

- ii. A higher brake thermal efficiency was obtained with WPO/WCO RCCI compared to G/D with up to 25 % increment at 1.06 bar BMEP due to increased peak pressure, higher heat release rate and better combustion phasing.
- iii. The HC and CO emissions decreased in WPO/WCO RCCI, particularly at low loads, with a maximum decrease of 54% and 48%, respectively.
- iv. The NO_x emissions obtained with WPO/WCO were higher than G/D RCCI, especially at low loads. NO_x emissions increased up to three times with WPO/WCO. However, it is significantly lower than in conventional diesel combustion.
- v. The maximum load achieved in PI-RCCI is up to 40% (2.12 bar BMEP) of the rated load. PI-RCCI is not realized at high-load operations owing to high pressure rise rates.
- vi. The lean premixed homogeneous combustion in PI-RCCI reduced the formation of HC and CO significantly. Compared with RCCI, HC and CO emissions are reduced by 48% and 45%, respectively, at 1.06 bar BMEP load in PI-RCCI.
- vii. The optimum WPOER ratio required to get maximum BTE is higher, with a maximum value of 75% in PI-RCCI than RCCI, to suppress early auto ignition and obtain optimal combustion phasing.
- viii. Smoke emissions have been reduced to near-zero levels in RCCI and PI-RCCI combustion.

The present study shows that fuels produced from waste resources can be effectively used in diesel engines with better performance and lower pollutant emissions by adopting PI-RCCI and RCCI strategies. However, long-term durability and material compatibility studies on utilizing WPO and WCO in diesel engines must be done before commercial implementation.

Acknowledgements

The authors gratefully acknowledge the funding for the present work by the Department of Science and Technology, Government of India, through the Indo-United Kingdom joint project, "Waste to Engine - Low Temperature Combustion of Sustainable Green Fuels" (Grant Number: DST_UKIERI - 2018-19-04).

References

- [1] S.D. Anuar Sharuddin, F. Abnisa, W.M.A. Wan Daud, M.K. Aroua, Energy recovery from pyrolysis of plastic waste: Study on non-recycled plastics (NRP) data as the real measure of plastic waste, *Energy Convers. Manag.* 148 (2017) 925–934.
<https://doi.org/10.1016/j.enconman.2017.06.046>.

- 1
2
3 [2] S.D. Anuar Sharuddin, F. Abnisa, W.M.A. Wan Daud, M.K. Aroua, A review on
4 pyrolysis of plastic wastes, *Energy Convers. Manag.* 115 (2016) 308–326.
5 <https://doi.org/10.1016/J.ENCONMAN.2016.02.037>.
6
7
8 [3] R. Miandad, M.A. Barakat, A.S. Aburiazza, M. Rehan, A.S. Nizami, Catalytic
9 pyrolysis of plastic waste: A review, *Process Saf. Environ. Prot.* 102 (2016) 822–838.
10 <https://doi.org/10.1016/j.psep.2016.06.022>.
11
12 [4] C. Areeprasert, J. Asingsamanunt, S. Srisawat, J. Kaharn, B. Inseemeeesak, P. Phasee,
13 C. Khaobang, W. Siwakosit, C. Chiemchaisri, Municipal Plastic Waste Composition
14 Study at Transfer Station of Bangkok and Possibility of its Energy Recovery by
15 Pyrolysis, *Energy Procedia.* 107 (2017) 222–226.
16 <https://doi.org/10.1016/j.egypro.2016.12.132>.
17
18 [5] D. Briassoulis, M. Hiskakis, E. Babou, S.K. Antiohos, C. Papadi, Experimental
19 investigation of the quality characteristics of agricultural plastic wastes regarding their
20 recycling and energy recovery potential, *Waste Manag.* 32 (2012) 1075–1090.
21 <https://doi.org/10.1016/j.wasman.2012.01.018>.
22
23 [6] H. Jeswani, C. Krüger, M. Russ, M. Horlacher, F. Antony, S. Hann, A. Azapagic, Life
24 cycle environmental impacts of chemical recycling via pyrolysis of mixed plastic
25 waste in comparison with mechanical recycling and energy recovery, *Sci. Total*
26 *Environ.* 769 (2021). <https://doi.org/10.1016/j.scitotenv.2020.144483>.
27
28 [7] S. Huang, H. Wang, W. Ahmad, A. Ahmad, N.I. Vatin, A.M. Mohamed, A.F. Deifalla,
29 I. Mehmood, Plastic Waste Management Strategies and Their Environmental Aspects:
30 A Scientometric Analysis and Comprehensive Review, 2022.
31 <https://doi.org/10.3390/ijerph19084556>.
32
33 [8] S.M. Al-Salem, A. Antelava, A. Constantinou, G. Manos, A. Dutta, A review on
34 thermal and catalytic pyrolysis of plastic solid waste (PSW), *J. Environ. Manage.* 197
35 (2017) 177–198. <https://doi.org/10.1016/J.JENVMAN.2017.03.084>.
36
37 [9] A.K. Das, S.S. Sahoo, A.K. Panda, Production of Plastic wastes Oil and Its Prospective
38 Use in a Variable Compression CI Engine, *J. Hazardous, Toxic, Radioact. Waste.* 25
39 (2021) 04021008. [https://doi.org/10.1061/\(ASCE\)HZ.2153-5515.0000606](https://doi.org/10.1061/(ASCE)HZ.2153-5515.0000606).
40
41 [10] A.K. Das, S.K. Sahu, A.K. Panda, Current status and prospects of alternate liquid
42 transportation fuels in compression ignition engines: A critical review, *Renew.*
43 *Sustain. Energy Rev.* 161 (2022) 112358. <https://doi.org/10.1016/j.rser.2022.112358>.
44
45 [11] G.T. Kalghatgi, The outlook for fuels for internal combustion engines, *Int. J. Engine*
46 *Res.* 15 (2014) 383–398. <https://doi.org/10.1177/1468087414526189>.
47
48
49
50
51
52
53
54
55
56
57
58
59
60

- 1
2
3 [12] R.D. Reitz, Directions in internal combustion engine research, *Combust. Flame*. 160
4 (2013) 1–8. <https://doi.org/10.1016/J.COMBUSTFLAME.2012.11.002>.
5
6 [13] S. Kimura, O. Aoki, Y. Kitahara, E. Aiyoshizawa, Ultra-clean combustion technology
7 combining a low-temperature and premixed combustion concept for meeting future
8 emission standards, *SAE Tech. Pap.* (2001). <https://doi.org/10.4271/2001-01-0200>.
9
10 [14] D.A. Splitter, R.D. Reitz, Fuel reactivity effects on the efficiency and operational
11 window of dual-fuel compression ignition engines, *Fuel*. (2014).
12
13 <https://doi.org/10.1016/j.fuel.2013.10.045>.
14
15 [15] H. Park, E. Shim, C. Bae, Expansion of low-load operating range by mixture
16 stratification in a natural gas-diesel dual-fuel premixed charge compression ignition
17 engine, *Energy Convers. Manag.* 194 (2019) 186–198.
18
19 <https://doi.org/10.1016/j.enconman.2019.04.085>.
20
21 [16] M. Murugesu Pandian, K. Anand, Comparison of different low temperature
22 combustion strategies in a light duty air cooled diesel engine, *Appl. Therm. Eng.* 142
23 (2018) 380–390. <https://doi.org/10.1016/j.applthermaleng.2018.07.047>.
24
25 [17] Y. Li, M. Jia, Y. Chang, M. Xie, R.D. Reitz, Towards a comprehensive understanding
26 of the influence of fuel properties on the combustion characteristics of a RCCI
27 (reactivity controlled compression ignition) engine, *Energy*. 99 (2016) 69–82.
28
29 <https://doi.org/10.1016/j.energy.2016.01.056>.
30
31 [18] M.M. Pandian, K. Anand, Experimental optimization of reactivity controlled
32 compression ignition combustion in a light duty diesel engine, *Appl. Therm. Eng.* 138
33 (2018) 48–61. <https://doi.org/10.1016/j.applthermaleng.2018.04.045>.
34
35 [19] S. Kokjohn, R. Hanson, D. Splitter, J. Kaddatz, R. Reitz, Fuel Reactivity Controlled
36 Compression Ignition (RCCI) Combustion in Light- and Heavy-Duty Engines, *SAE*
37 *Int. J. Engines*. 4 (2011) 360–374. <https://doi.org/10.4271/2011-01-0357>.
38
39 [20] K. Anand, R.D. Reitz, E. Kurtz, W. Willems, Modeling Fuel and EGR effects under
40 conventional and low temperature combustion conditions, *Energy and Fuels*. 27 (2013)
41 7827–7842. <https://doi.org/10.1021/ef401989c>.
42
43 [21] J. Benajes, J. V. Pastor, A. García, J. Monsalve-Serrano, The potential of RCCI
44 concept to meet EURO VI NO_x limitation and ultra-low soot emissions in a heavy-
45 duty engine over the whole engine map, *Fuel*. (2015).
46
47 <https://doi.org/10.1016/j.fuel.2015.07.064>.
48
49 [22] L. Zhu, Y. Qian, X. Wang, X. Lu, Effects of direct injection timing and premixed ratio
50 on combustion and emissions characteristics of RCCI (Reactivity Controlled
51
52
53
54
55
56
57
58
59
60

- 1
2
3 Compression Ignition) with N-heptane/gasoline-like fuels, *Energy*. 93 (2015) 383–392.
4 <https://doi.org/10.1016/j.energy.2015.09.069>.
- 5
6 [23] J. Benajes, S. Molina, A. García, J. Monsalve-Serrano, Effects of direct injection
7 timing and blending ratio on RCCI combustion with different low reactivity fuels,
8 *Energy Convers. Manag.* (2015). <https://doi.org/10.1016/j.enconman.2015.04.046>.
- 9
10 [24] S.H. Park, D. Shin, J. Park, Effect of ethanol fraction on the combustion and emission
11 characteristics of a dimethyl ether-ethanol dual-fuel reactivity controlled compression
12 ignition engine, *Appl. Energy*. 182 (2016) 243–252.
13 <https://doi.org/10.1016/j.apenergy.2016.07.101>.
- 14
15 [25] V.B. Pedrozo, I. May, M. Dalla Nora, A. Cairns, H. Zhao, Experimental analysis of
16 ethanol dual-fuel combustion in a heavy-duty diesel engine: An optimization at low
17 load, *Appl. Energy*. 165 (2016) 166–182.
18 <https://doi.org/10.1016/j.apenergy.2015.12.052>.
- 19
20 [26] Z. Jia, I. Denbratt, Experimental investigation into the combustion characteristics of a
21 methanol-Diesel heavy duty engine operated in RCCI mode, *Fuel*. 226 (2018) 745–
22 753. <https://doi.org/10.1016/j.fuel.2018.03.088>.
- 23
24 [27] D.Z. Zhou, W.M. Yang, H. An, J. Li, C. Shu, A numerical study on RCCI engine
25 fueled by biodiesel/methanol, *Energy Convers. Manag.* 89 (2015) 798–807.
26 <https://doi.org/10.1016/j.enconman.2014.10.054>.
- 27
28 [28] M. Mohebbi, M. Reyhanian, V. Hosseini, M.F. Muhamad Said, A.A. Aziz,
29 Performance and emissions of a reactivity controlled light-duty diesel engine fueled
30 with n-butanol-diesel and gasoline, *Appl. Therm. Eng.* 134 (2018) 214–228.
31 <https://doi.org/10.1016/J.APPLTHERMALENG.2018.02.003>.
- 32
33 [29] S.K. Gupta, K. Anand, Experimental investigations to reduce unburned emissions in
34 reactivity controlled compression ignition through fuel modifications, *Appl. Therm.*
35 *Eng.* 146 (2019) 622–634. <https://doi.org/10.1016/j.applthermaleng.2018.10.036>.
- 36
37 [30] M. Mohebbi, M. Reyhanian, V. Hosseini, M.F. Muhamad Said, A.A. Aziz,
38 Performance and emissions of a reactivity controlled light-duty diesel engine fueled
39 with n-butanol-diesel and gasoline, *Appl. Therm. Eng.* 134 (2018) 214–228.
40 <https://doi.org/10.1016/j.applthermaleng.2018.02.003>.
- 41
42 [31] S. Pan, X. Li, W. Han, Y. Huang, An experimental investigation on multi-cylinder
43 RCCI engine fueled with 2-butanol/diesel, *Energy Convers. Manag.* 154 (2017) 92–
44 101. <https://doi.org/10.1016/j.enconman.2017.10.047>.
- 45
46 [32] J. Cha, S. Kwon, S. Kwon, S. Park, Combustion and emission characteristics of a
47
48
49
50
51
52
53
54
55
56
57
58
59
60

- 1
2
3 gasoline-dimethyl ether dual-fuel engine, Proc. Inst. Mech. Eng. Part D J. Automob.
4 Eng. 226 (2012) 1667–1677. <https://doi.org/10.1177/0954407012450122>.
5
6
7 [33] G. Duraisamy, M. Rangasamy, N. Govindan, A comparative study on methanol/diesel
8 and methanol/PODE dual fuel RCCI combustion in an automotive diesel engine,
9 Renew. Energy. 145 (2020) 542–556. <https://doi.org/10.1016/j.renene.2019.06.044>.
10
11 [34] J. Hwang, C. Bae, T. Gupta, Application of waste cooking oil (WCO) biodiesel in a
12 compression ignition engine, Fuel. 176 (2016) 20–31.
13
14 <https://doi.org/10.1016/j.fuel.2016.02.058>.
15
16
17 [35] A.R. Chidambaram, A. Krishnasamy, Investigations on Dual Fuel Reactivity
18 Controlled Compression Ignition Engine using Alternative Fuels Produced from Waste
19 Resources, SAE Tech. Pap. (2022) 1–11. <https://doi.org/10.4271/2022-01-1095>.
20
21
22 [36] S.I.I.N.A. Small-bore, M. Engine, M.L. Wissink, S.J. Curran, ICEF2017-3607
23 OPERATING WITH REACTIVITY-CONTROLLED COMPRESSION IGNITION,
24 (2017) 1–9.
25
26
27
28
29
30
31
32
33
34
35
36
37
38
39
40
41
42
43
44
45
46
47
48
49
50
51
52
53
54
55
56
57
58
59
60